INTELLIGENT SYSTEMS FOR OPTICAL FORM MEASUREMENT: AUTOMATED ASSESSMENT OF POSE AND COVERAGE

Sofia Catalucci[1], Nicola Senin[1,2], Samanta Piano[1], Richard Leach[1]
[1]Manufacturing Metrology Team, Faculty of Engineering
University of Nottingham
Nottingham, United Kingdom
[2]Department of Engineering
University of Perugia
Perugia, Italy

INTRODUCTION

This work addresses the development of intelligent and adaptive optical form measurement systems for quality inspection of additively manufactured complex parts. The ultimate objective is to obtain smart optical measurement systems capable of automatically reconfiguring themselves while inspecting new geometries, and capable of assessing whether completed measurements are sufficient, or further measurements should be performed. Intelligent behaviour is achieved through automated self-assessment of measurement performance, while the measurement itself is being executed [1]. The decisional process is supported by multiple sources of information [2], namely: knowledge of part specifications (CAD model, dimensional and geometric tolerances, materials); knowledge of the manufacturing process and the material, leading to predictability of likely types of form error; knowledge of the measurement instrument itself (metrological performance and behaviour), and how it is expected to interact with any specific material and part geometry. The optical measurement technologies covered by the project produce point clouds: the work presented in this paper focuses on algorithmic processing of point clouds, and deals with the following, specific challenges: a) automated point cloud localisation within the part geometry, i.e. identifying what surfaces have been captured by any given point cloud, acquired from a part of unknown position and orientation; b) automated assessment of coverage and sampling density for the exposed surfaces, including recognition of critical regions (i.e. poorly represented by the point cloud), in order to support automated planning for further measurements.

TEST SET UP

The experimental set-up is based on a combination of a commercial measurement fringe projection system (blue-light technology GOM Atos Core 300), shown in Figure 1, and the point cloud processing commercial software Polyworks Inspector by Innovmetric. Automation is achieved by interfacing Polyworks with MATLAB, via scripting.

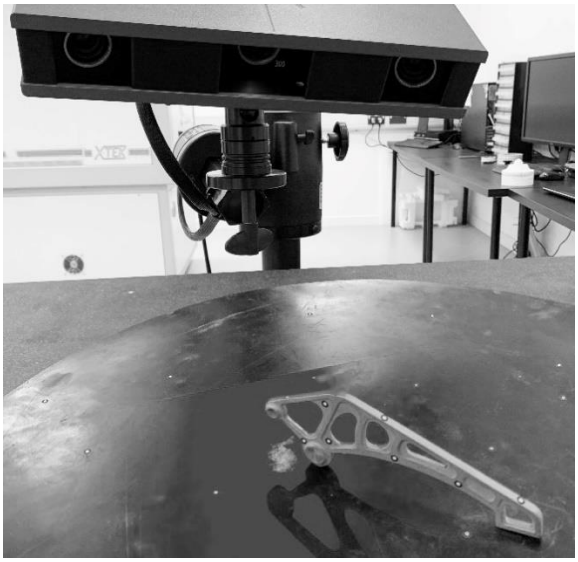

FIGURE 1. The optical measurement system while measuring one of the test parts.

Test cases

The selected test measurement parts are shown in Figure 2. Sample A (Figure 2a) was fabricated by selective laser sintering (SLS) using Nylon 12, with size of a rectangular enclosing envelope (50 × 50 × 28) mm; sample B (Figure 2b) was fabricated by laser powder bed fusion (LPBF) using stainless steel 316L, with dimensions of (125 × 45 × 8) mm.

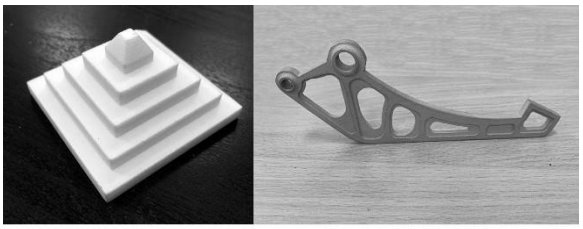

a) b)

FIGURE 2. Test parts; a) Nylon 12 pyramid sample (50 × 50 × 28) mm fabricated by SLS; b) stainless steel 316L automotive sample (125 × 45 × 8) mm fabricated by LPBF.

The nominal geometries of the test parts are available as triangle meshes. Example results of single measurements on the test parts with unknown pose are shown in Figure 3a for sample A and Figure 3b for sample B.

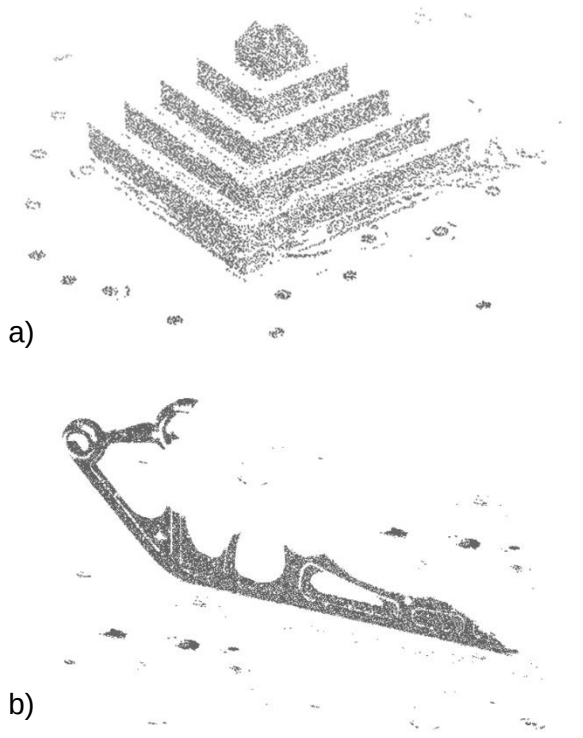

a)

b)

FIGURE 3. Example measurements: a) sample A; b) sample B.

As sample A has four nominally identical sides, pose estimation only pertains to the accurate identification of the angular orientation of the visible corner in the point cloud.

DATA PROCESSING METHOD

The first data processing step consists of detecting the pose by identification and best-matching of landmark features present on both the measured point cloud and the nominal reference geometry (triangle mesh). In the second step, once the point cloud has been aligned to the mesh, the degree of coverage can be assessed by identifying the surfaces that have not been reached by the measurement instrument. For the covered surfaces, the density and spatial distribution of the measured points can be computed by inspecting the positions of the points falling within each triangle of the mesh.

STEP 1: ALIGNMENT

Alignment, also referred to as registration, consists of a coarse phase and a fine phase.

Coarse registration

Coarse registration is based on the identification and matching of common landmarks both in the measured point cloud and in the triangle mesh. Landmarks can be identified through computation of local feature descriptors [3-5]. In this work, local curvatures are used.

Surface normal vectors are identified both on the point cloud and in the triangle mesh, by using principal component analysis [6] on local subsets of neighbouring points selected via the *k*-nearest neighbour algorithm [7]. The principal curvatures $k1$ and $k2$ are then computed [8]. From the principal curvatures, the Gaussian curvature *K* and mean curvature *H* are computed as follows:

$$K = k1 \cdot k2, \quad (1)$$

$$H = \frac{(k1 + k2)}{2}. \quad (2)$$

Example results for curvature are shown in Figures 4 to 7.

The next step involves the identification of clusters of points with similar curvature values: a first *k*-means clustering process [9] was used to identify *k*-classes of curvature values (*k* = 5). The highest-curvature class was then isolated; the resulting points were subjected to another clustering process, this time aimed at isolating spatially distant subsets of points with high-curvature values. The second clustering was, therefore, hierarchical and based on Euclidean distances between points (Figures 8 to 11).

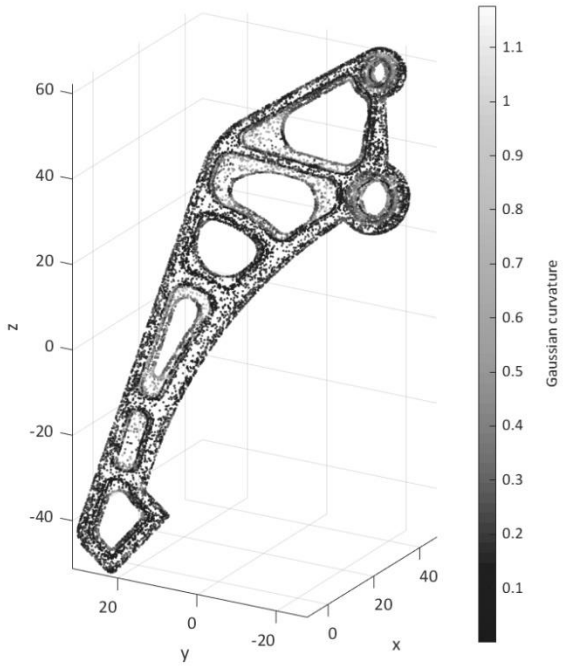

FIGURE 4. Gaussian curvature K estimation on extracted vertices of the triangle mesh (sample B).

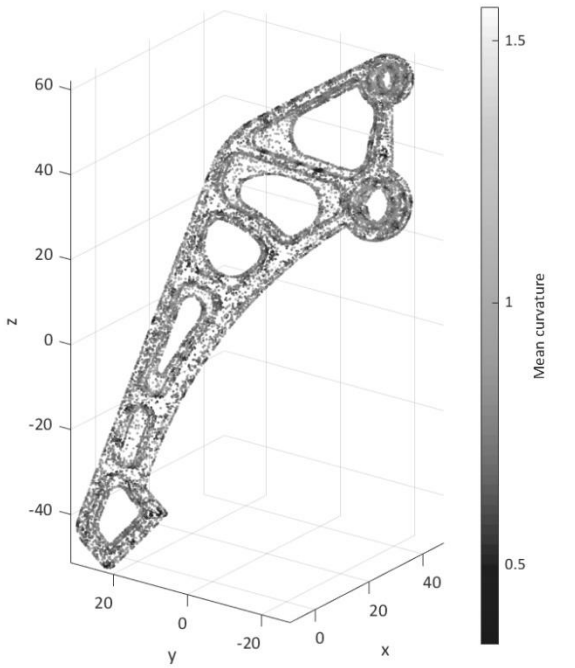

FIGURE 5. Mean curvature H estimation on extracted vertices of the triangle mesh (sample B).

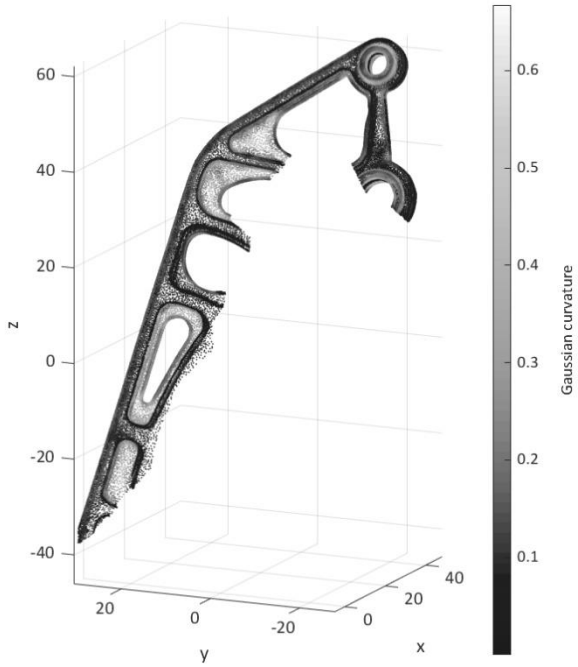

FIGURE 6. Gaussian curvature K estimation on point cloud dataset (sample B).

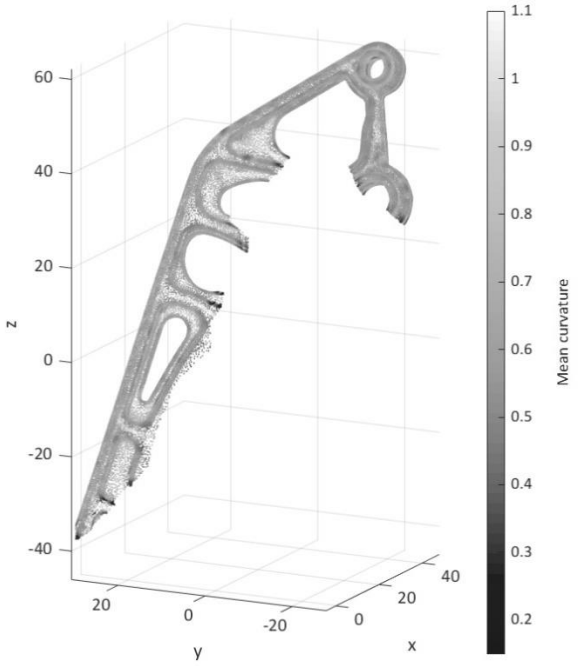

FIGURE 7. Mean curvature H estimation on point cloud dataset (sample B).

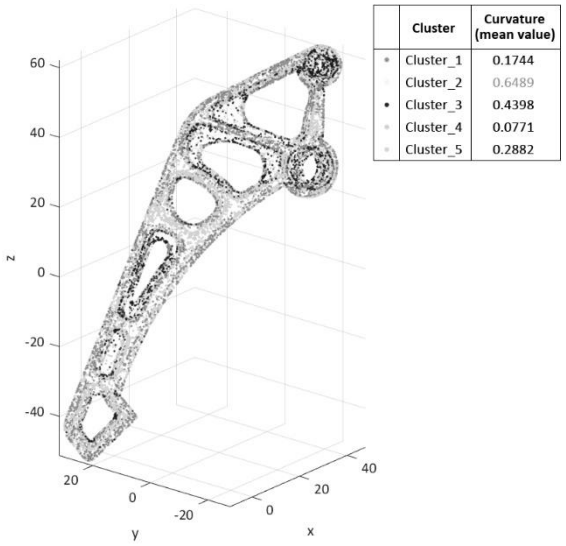

FIGURE 8. k-means clustering on K curvature. Cluster 2 refers to the extracted vertices of the triangle mesh with the highest curvature values (sample B).

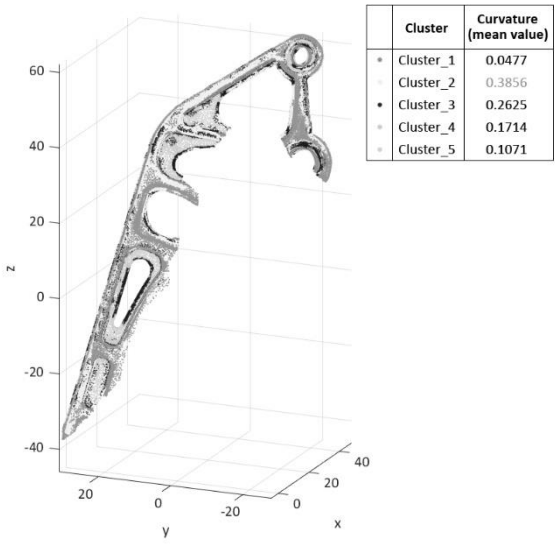

FIGURE 10. k-means clustering on K curvature. Cluster 2 refers to the points with the highest curvature values (sample B).

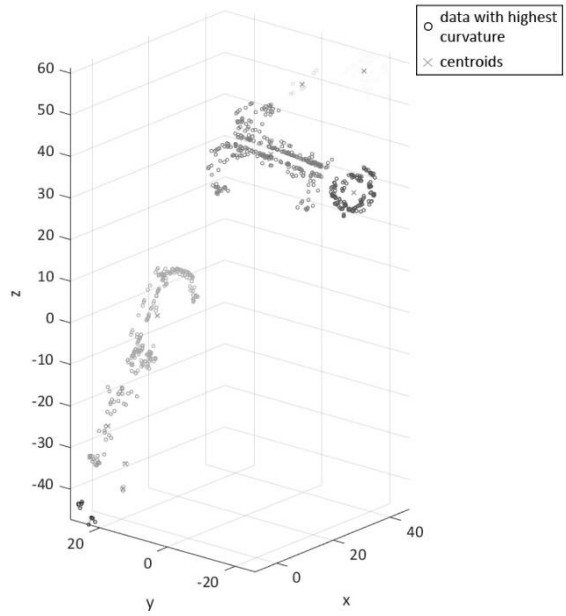

FIGURE 9. Hierarchical clustering and centroids computation of clustered extracted vertices of the triangle mesh (sample B). The points taken into account are the ones with the highest curvature values.

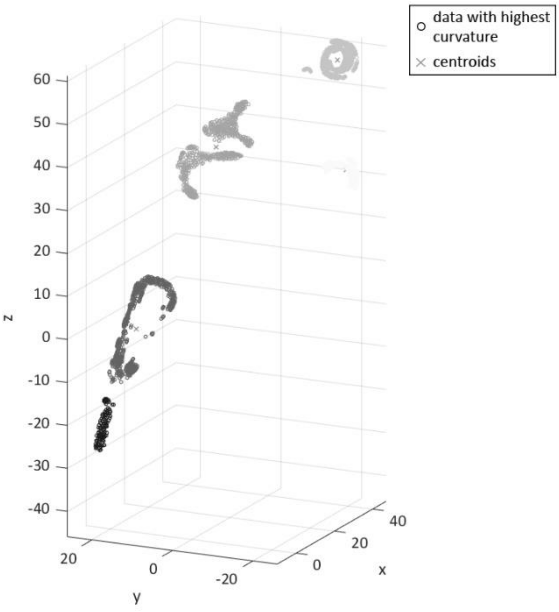

FIGURE 11. Hierarchical clustering and centroids computation of clustered point cloud (sample B). The points taken into account are the ones with the highest curvature values.

The identified common landmarks in both datasets, described by high curvature values, are then best-matched, using Random sample consensus (RANSAC) [10,11]: at each iteration, good matches were considered those resulting in a spatial alignment which minimises the sum of squared distances between matched points, using the Procrustes algorithm [12].

Fine registration

Fine registration is based on a best-fit algorithm [15], which iteratively minimises the distances from the measured dataset to the reference entity, revising the transformation based on a rigid transformation (translation and rotation) until the variation of the squared error is minimised. The “registration error function” is defined as the sum of squared Euclidean distances between each point in the cloud and its closest neighbour located on the triangular facets [13].

COVERAGE ASSESSMENT

After the fine registration process is completed, each triangular facet belonging to the original mesh will have a certain number of measured points associated with it. Coverage expresses how comprehensively each triangle is represented by the associated measured points. To assess coverage, the number of points falling within each triangle is considered in relation to the area of the triangle with the purpose to obtain a measure of spatial sampling density, i.e. number of points per unit area. Sampling density is computed on all the triangles (Figure 12). Then, a percentage of the maximum density is set as threshold to discriminate between adequately and inadequately covered triangles (simply referred to as "uncovered"). Finally, a coverage ratio can be defined as the percentage of triangles with adequate coverage over the total number of triangles in the mesh. Additionally, the ratio between the total area occupied by triangles classified as covered, and the total area of all the triangles in the mesh, can be computed, and is referred to as "covered area ratio".

Example results of coverage computation are shown in Figures 13 to 14, where the threshold has been set to 75% of the maximum sampling density per triangle. The areal coverage is either estimated based on the number of triangular facets associated with measured points over the total number of triangles, and the sum of the covered area over the total area of the object (Table 1).

FIGURE 12. Triangle facets; colouring proportional to sampling density (sample B).

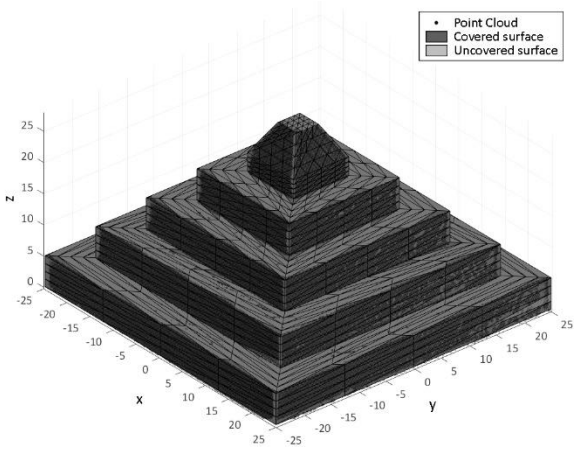

FIGURE 13. Covered and uncovered triangles for sample A (threshold on sampling density at 75%).

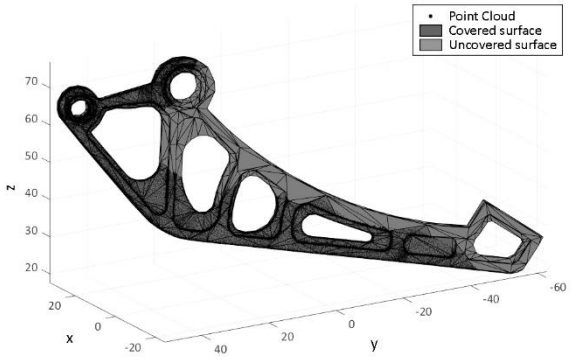

FIGURE 14. Covered and uncovered triangles for sample B (threshold on sampling density at 75%).

TABLE 1. Coverage ratio results.

	No. of triangles in the mesh	Coverage ratio (% covered triangles)	Covered area ratio (% covered area)
Sample A	1344	22%	32%
Sample B	1785	39%	42%

CONCLUSIONS AND FUTURE WORK

In this paper, preliminary results from the early stage development of an intelligent system for complex shape measuring have been presented. Methods and algorithms for the automatic assessment of part pose and measurement coverage have been introduced and discussed with the support of two test cases. The prototype implementation is realised using a combination of commercial measurement hardware and software, and custom software modules developed in-house.

Future work will address: 1) the estimation of uncertainty associated with alignment and assessment of coverage. Alignment in particular may be affected by problems of geometric stability (e.g. see [14] for ICP); 2) the differentiation of part surfaces depending on functional relevance, so that assessment of coverage quality can be weighed; 3) the implementation of feedback mechanisms based on the results of pose and coverage estimation, to automate planning for further measurement actions.

ACKNOWLEDGEMENTS

The authors would like to acknowledge Patrick Bointon of the Manufacturing Metrology Team, Leonidas Gargalis and Joe White of the Centre for Additive Manufacturing, University of Nottingham, for their assistance in designing and producing the test cases. We also acknowledge funding from EPRSC project EP/M008983/1.

REFERENCES

[1] Stavroulakis P, Chen S, Derlome C, Bointon P, Tzimiropoulos G, Leach R K. Rapid calibration tracking of extrinsic projector parameters in fringe projection using machine learning. Opt. Lasers Eng. 2019; 114: 7-14.

[2] Senin N, Leach R K. Information-rich surface metrology. Proc. CIRP. 2018; 75: 19-26.

[3] Hana X F, Jin J S, Xie J, Wang M J, Jiang W. A comprehensive review of 3D point cloud descriptors. 2018; arXiv:1802.02297.

[4] Tombari F, Salti S, Di Stefano L. Unique signatures of histograms for local surface description. European conference on computer vision. Springer; 2010. 356-369.

[5] Bellekens B, Spruyt V, Berkvens R, Penne R, Weyn M. A benchmark survey of rigid 3d point cloud registration algorithms. Inter. Journ. Adv. Intell. Sysm. 2015.

[6] Chung D, Lee Y DS. Registration of multiple-range views using the reverse-calibration technique. Pattern Recogn. 1998; 31: 457-464.

[7] Friedman J H, Bentely J, Finkel R A. An Algorithm for Finding Best Matches in Logarithmic Expected Time. ACM Transactions on Mathematical Software. 1977; 3: 209-226.

[8] Merigot Q, Ovsjanikov M, Guibas L J. Voronoi-based curvature and feature estimation from point clouds. Visualization and Computer Graphics, IEEE Transactions on. 2011; 17: 743-756.

[9] Ding C, He X. K-means clustering via Principal Component Analysis. Proceedings of International Conference on Machine Learning. 2004. 225-232.

[10] Moretti M, Gambucci G, Leach R K, Senin N. Assessment of surface topography modifications through feature-based registration of areal topography data. Surf. Topogr. Metrol. Prop. 2019; 7.

[11] Fishler M A, Bolles R C. Random sample consensus: A paradigm for model fitting with applications to image analysis and automated cartography. Commun. ACM. 1981; 24: 381-95.

[12] Kendall D G. A survey of the statistical theory of shape. Statistical Science. 1989; 4: 87-99.

[13] Besl P, McKay N. A method for registration of 3-D shapes. IEEE TPAMI. 1992; 14: 239-256.

[14] Gelfand N, Ikemoto L, Rusinkiewicz S, Levoy M. Geometrically stable sampling for the ICP algorithm. Proceedings of International Conference on 3-D Digital Imaging and Modeling, 3DIM. 2003.